

## One-phonon isovector $2_{1,MS}^+$ state in the neutron-rich nucleus $^{132}\text{Te}$

M. Danchev,<sup>1</sup> G. Rainovski,<sup>1,2</sup> N. Pietralla,<sup>2,3</sup> A. Gargano,<sup>4</sup> A. Covello,<sup>4,5</sup> C. Baktash,<sup>6</sup> J. R. Beene,<sup>6</sup> C. R. Bingham,<sup>7</sup> A. Galindo-Uribarri,<sup>6</sup> K. A. Gladnishki,<sup>1</sup> C. J. Gross,<sup>6</sup> V. Yu. Ponomarev,<sup>2</sup> D. C. Radford,<sup>6</sup> L. L. Riedinger,<sup>7</sup> M. Scheck,<sup>2</sup> A. E. Stuchbery,<sup>8</sup> J. Wambach,<sup>2</sup> C.-H. Yu,<sup>6</sup> and N. V. Zamfir<sup>9</sup>

<sup>1</sup>Faculty of Physics, St. Kliment Ohridski University of Sofia, BG-1164 Sofia, Bulgaria

<sup>2</sup>Institut für Kernphysik, TU Darmstadt, D-64289 Darmstadt, Germany

<sup>3</sup>GSI Helmholtzzentrum für Schwerionenforschung, D-64291 Darmstadt, Germany

<sup>4</sup>Istituto Nazionale di Fisica Nucleare, Complesso Universitario di Monte S. Angelo, Via Cintia, I-80126 Napoli, Italy

<sup>5</sup>Dipartimento di Scienze Fisiche, Università di Napoli - Federico II, Complesso Universitario di Monte S. Angelo, Via Cintia, I-80126 Napoli, Italy

<sup>6</sup>Physics Division, ORNL, Oak Ridge, Tennessee 37831, USA

<sup>7</sup>Department of Physics and Astronomy, University of Tennessee, Knoxville, Tennessee 37996, USA

<sup>8</sup>Department of Nuclear Physics, ANU, Canberra, ACT 0200, Australia

<sup>9</sup>Wright Nuclear Structure Laboratory, Yale University, New Haven, Connecticut 06520-8124, USA

(Received 10 October 2011; published 27 December 2011)

The  $2_2^+$  state in  $^{132}\text{Te}$  is identified as the one-phonon mixed-symmetry state in a projectile Coulomb excitation experiment presenting a firm example of a mixed-symmetry state in unstable, neutron-rich nuclei. The results of shell-model calculations based on the low-momentum interaction  $V_{\text{low}-k}$  are in good agreement with experiment demonstrating the ability of the effective shell-model interaction to produce states of mixed-symmetry character.

DOI: [10.1103/PhysRevC.84.061306](https://doi.org/10.1103/PhysRevC.84.061306)

PACS number(s): 21.10.Re, 23.20.Js, 25.70.De, 27.60.+j

Neutron-rich nuclei in the vicinity of double-magic-shell closures away from the line of stability are currently of great interest. This interest is motivated by the endeavor to understand the nuclear many-body system at extreme neutron excess and fueled by new experimental data which have become available in recent years due to the progress made in the production of radioactive ion beams (RIBs). On the journey toward the neutron drip line one needs a reliable theoretical model which incorporates the known features of the nuclear many-body system and has enough predictive power for a wide range of nuclei. The nuclear shell model provides the basic framework for understanding the detailed structure of complex nuclei as arising from the individual motion of nucleons and the effective nuclear interaction between them. In this model, nuclei with a few nucleons outside doubly closed shells play a special role. They provide direct information on the single-particle energies and the best testing ground for different components of the effective interaction.

In this context, a good example is given by  $^{136}\text{Te}$  where a reduction of both the  $E_x(2_1^+)$  and the  $B(E2; 2_1^+ \rightarrow 0_1^+)$  with respect to the lighter isotopes is observed [1]. This simultaneous decrease clearly violates the empirical rules for properties of quadrupole collective states [2,3]. In addition, the fact that the  $B(E2; 2_1^+ \rightarrow 0_1^+)$  in  $^{136}\text{Te}$  is significantly lower than the one in  $^{132}\text{Te}$  implies a considerable difference between the structures of the  $2_1^+$  states in these nuclei. As matter of fact, it is suggested [4–6] that neutron dominance in the wave function of the  $2_1^+$  state in  $^{136}\text{Te}$  is the main reason for the observed peculiar properties. This proton-neutron asymmetry is a combined effect of the asymmetry in the excitation energies of the basic  $2^+$  proton [ $E_x(2_1^+; ^{134}\text{Te}) = 1279$  keV] and neutron [ $E_x(2_1^+; ^{134}\text{Sn}) = 762$  keV] configurations and the weak proton-neutron interaction which cannot compensate

for the above energy difference [5]. The situation in  $^{132}\text{Te}$  is quite different; the excitation energy of the basic neutron  $2^+$  configuration in  $^{132}\text{Te}$  [ $E_x(2_1^+; ^{130}\text{Sn}) = 1221$  keV] is comparable to the excitation energy of the basic proton  $2^+$  configuration. This suggests that the  $2_1^+$  state of  $^{132}\text{Te}$  has a more balanced proton-neutron character than that of  $^{136}\text{Te}$ , which leads to a  $B(E2; 2_1^+ \rightarrow 0_1^+)$  value in agreement with the expected trends. A direct proof for the above scenario might come from a comparison of the magnetic moments of the  $2_1^+$  states in  $^{132}\text{Te}$  [7–9] and  $^{136}\text{Te}$ . Another way to investigate the proton-neutron balance of the wave function is based on the decay properties of the isovector analog of the  $2_1^+$  state [10], the one-phonon state with mixed proton-neutron symmetry  $2_{1,MS}^+$  [11]. The one-phonon  $2^+$  vibrational states in even-even nuclei are the simplest collective excitations. Due to the two-fluid nature of nuclear matter they appear as a symmetric [the one-phonon  $2_1^+$  fully symmetric state (FSS)] or an antisymmetric combination of the involved proton and neutron configurations. Because of its isovector nature the  $2_{1,MS}^+$  state decays with a strong  $M1$  transition to the one-phonon FSS and with a weak  $E2$  transition to the ground state. This unique decay serves as an experimental fingerprint for the  $2_{1,MS}^+$  state. In the framework of IBM-2 [11] the one-phonon FS and mixed-symmetry state (MSS) are orthogonal states, built on the same microscopic configurations. Moreover, it has been shown that the absolute  $B(M1; 2_{1,MS}^+ \rightarrow 2_1^+)$  strength is highly sensitive to the proton-neutron balance of the wave functions through a mechanism dubbed configurational isospin polarization (CIP) [12]. The CIP mechanism and its manifestations have been experimentally confirmed in  $^{92}\text{Zr}$  [13]. The case of significant CIP, which can be expected in  $^{136}\text{Te}$ , should be manifested by comparatively small absolute  $M1$  rates. The opposite case of vanishing CIP can be expected

in  $^{132}\text{Te}$  which leads to a strong  $M1$  transition between the one-phonon MS and FSSs. Apparently, the CIP of one-phonon MS and FSSs in  $^{132}\text{Te}$  and  $^{136}\text{Te}$  allows the proton-neutron balance in their wave functions to be studied by measuring and comparing their absolute  $B(M1; 2_{1,\text{MS}}^+ \rightarrow 2_1^+)$  values.

Information on MSSs is relatively scarce [14]. This is particularly true for the mass  $A \approx 130$  region where until recently only a few MSSs were known on the basis of observed strong  $M1$  decays [15–17]. However in the last several years the number of identified MSSs in this mass region has increased substantially; by using projectile Coulomb excitation reactions and the Gammasphere array at Argonne National Laboratory, the one-phonon MSSs were identified in several low-abundance stable nuclei, namely  $^{134}\text{Xe}$  [18],  $^{138}\text{Ce}$  [19],  $^{136}\text{Ce}$  [20], and  $^{130,132}\text{Xe}$  [21]. This experimental technique is considered to be applicable for identification of MSSs of RIBs but this has not been demonstrated in practice, yet. There have already been a few unsuccessful experimental attempts to identify one-phonon MSSs in neutron-rich nuclei using various experimental techniques [22,23]. This leaves still open the question: What is the appropriate technique to identify and study the properties of MSSs in radioactive nuclei? *No MSSs have yet been solidly identified in unstable nuclei on the basis of large absolute  $M1$  transition rates.*

The new experimental data on MSSs in the stable  $N = 80$  isotones have revealed their evolution with increasing proton number which allows a prediction for the energy of the one-phonon MSS in the  $^{132}\text{Te}$  to be made [18]. The fit procedure [24] used in Ref. [18] suggests the  $2_2^+$  level in  $^{132}\text{Te}$  at 1665 keV as a candidate for the one-phonon MSS. Shell-model calculations [25] have corroborated this prediction.

In this study we report on the first firm experimental identification of a one-phonon MSS in the neutron-rich unstable nucleus  $^{132}\text{Te}$ , demonstrating that the projectile Coulomb excitation of RIBs is the proper experimental technique to study the MSSs in exotic nuclei. The observed strong  $B(M1; 2_{1,\text{MS}}^+ \rightarrow 2_1^+)$  value is in agreement with the expectations for vanishing CIP which is also confirmed by the shell-model calculations we performed.

$^{132}\text{Te}$  is one of the first radioactive neutron-rich nuclei in which the  $B(E2; 2_1^+ \rightarrow 0_1^+)$  value was measured in projectile Coulomb excitation reactions of a RIB [1]. The excited states of  $^{132}\text{Te}$  have been identified in a  $\gamma$ - $\gamma$  measurement following the  $\beta^-$  decay of  $^{132}\text{Sb}$  [26]. The second excited state at 1665.3 keV discovered in the latter study decays predominantly to the  $2_1^+$  state by a 690.9 keV transition and to the ground state by a very weak 1665.3 keV transition [ $I_\gamma(691 \text{ keV})/I_\gamma(1665 \text{ keV}) = 100(52)$ ]. The observed intensity dominance of the decay to the  $2_1^+$  state relative to the high-energy decay to the  $0_1^+$  ground state is typical for the decay of a  $2_{1,\text{MS}}^+$  state due to its large  $B(M1; 2_{1,\text{MS}}^+ \rightarrow 2_1^+)$  value. The magnetic moment of the  $2_1^+$  state in  $^{132}\text{Te}$  has been determined experimentally by using the technique of recoil in vacuum (RIV) after a projectile Coulomb excitation reaction on a carbon target [7]. Providing that states above the  $2_1^+$  are also populated in this experiment, their relative  $\gamma$ -ray yields with respect to the  $2_1^+$  state measure the relative Coulomb excitation cross-sections. This experimental information, in combination with the known  $B(E2; 0_1^+ \rightarrow 2_1^+)$  value [1], can give the decay

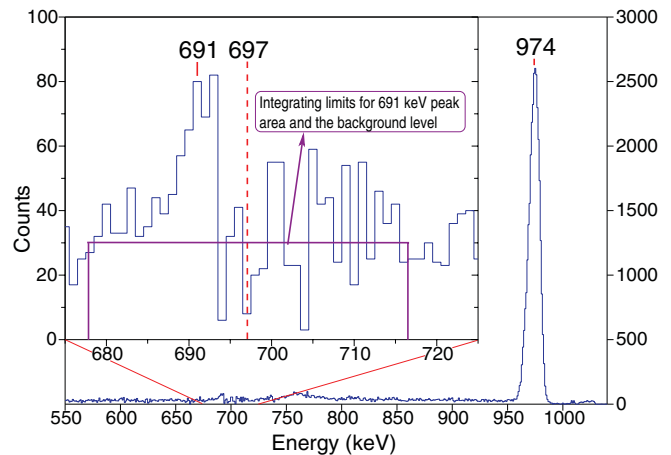


FIG. 1. (Color online) Doppler-corrected, background-subtracted spectrum of all  $\gamma$  rays observed in coincidence with  $^{12}\text{C}$  recoils detected in HyBall. For details see the text. The inset shows the existence and the integration of the peak area of 691-keV transition. Background level is the averaged counts between 570 and 645 keV, where the Compton continuum of 974-keV peak is relatively flat.

strength in the same manner as was demonstrated in the case of stable nuclei [18–21]. This information eventually could reveal the character of the  $2_2^+$  state in  $^{132}\text{Te}$ . With this idea in mind we have reevaluated the data from the experiment described in Ref. [7].

The experiment was carried out at the HRIBF Facility at Oak Ridge National Laboratory. The  $^{132}\text{Te}$  RIB was accelerated to 3 MeV/u and Coulomb-excited on a thick self-supporting  $^{12}\text{C}$  target. The data were acquired for 64 hours with a beam intensity of about  $3 \times 10^7$  pps.  $\gamma$  rays resulting from Coulomb excitation and decay of  $^{132}\text{Te}$  nuclei were detected with the CLARION array [27].  $^{12}\text{C}$  ions scattered out of the target were detected in the HyBall array [27]. The used rings in HyBall covered carbon scattering angles between  $7^\circ$  and  $44^\circ$  [7].  $\gamma$  rays observed in coincidence with the  $^{12}\text{C}$  ions detected in HyBall were corrected for Doppler shift. In order to reduce the background from uncorrelated CLARION-HyBall coincidences, the time difference between CLARION and HyBall was projected and the  $\gamma$  spectrum from the gate set on uncorrelated events was subtracted from the  $\gamma$  spectrum from the gate set on correlated events. This procedure yields the  $\gamma$ -ray spectrum shown in Fig. 1. In this spectrum all  $\gamma$  rays from the radioactive decays of the beam are completely subtracted. Besides the 974-keV transition, which dominates the spectrum and represents the decay of the  $2_1^+$  state, we also have observed a  $\gamma$  ray with energy of 691 keV (see the inset in Fig. 1). This peak is sharp and well pronounced, which indicates that it is emitted in flight with a speed and direction equal to those of the excited  $^{132}\text{Te}$  ions. From this observation, together with the coincidence conditions and the background subtraction procedure, it is clear that the 691-keV  $\gamma$  line represents the decay of a low-lying Coulomb-excited state of  $^{132}\text{Te}$ . Indeed, a  $\gamma$  ray with this energy is known [26] in the decay scheme of  $^{132}\text{Te}$ . It represents the  $(2_2^+) \rightarrow 2_1^+$  transition. As seen in Fig. 1 the 691 keV line is certainly not the known 697 keV  $4^+ \rightarrow 2^+$

transition [26]. The 1665-keV level was tentatively assigned spin parity  $2^+$  in Ref. [26] on the basis of observed decay to the  $2_1^+$  and  $0_1^+$  states. Given the observation of the 1665-keV level under the present experimental conditions, the only possible spin-parity assignment for it is  $2^+$ .

From the peak areas of the 974-keV [ $N = 30400(500)$ ] and the 691-keV [ $N = 354(102)$ ] transitions obtained from the spectrum in Fig. 1 and the reported branching ratio for the decay of the  $2_2^+$  state [26] the relative population of the  $2_2^+$  state with respect to the population of the  $2_1^+$  state is  $1.01(28) \times 10^{-2}$ . It measures the relative Coulomb excitation (CE) cross sections. Erroneous target thickness was reported in Refs. [1,7]. The correct thickness of the target in both references was  $1.13(6) \text{ mg/cm}^2$ . As a consequence, the values for the  $B(E2; 0_1^+ \rightarrow 2_1^+)$  in  $^{132,134,136}\text{Te}$  given in Table II of Ref. [1] should read  $0.216(22) \text{ e}^2\text{b}^2$ ,  $0.114(13) \text{ e}^2\text{b}^2$ ,  $0.122(18) \text{ e}^2\text{b}^2$ , respectively. The new value for the  $B(E2; 0_1^+ \rightarrow 2_1^+)$  in  $^{132}\text{Te}$  influences the adopted value for the lifetime of the  $2_1^+$  state and consequently the value for its magnetic moment deduced in Refs. [7,8]. From the reevaluated lifetime of the  $2_1^+$  state [ $\tau = 2.2(5) \text{ ps}$ ] and using the RIV calibration from [8] we find  $g(2_1^+) = (+)0.46(5)$ . We stress that these new values do not qualitatively affect the phenomenon of lowering the  $B(E2)$  value in  $^{136}\text{Te}$  and its consequences as discussed above and in Ref. [1]. The experimental relative population of the  $2_2^+$  state was fitted to the Winther–de Boer theory using a multiple CE code [28] and taking into account the energy loss of the beam in the target ( $\sim 80 \text{ MeV}$ ). Absolute cross-sections were derived using the new value  $B(E2; 0_1^+ \rightarrow 2_1^+) = 0.216(22) \text{ e}^2\text{b}^2$  and the branching ratio for the decay of the  $2_2^+$  state [26].

The combination of the Coulomb excitation yields, the known decay branching ratio, and the fact that the  $B(E2; 2_2^+ \rightarrow 2_1^+)$  value is extremely unlikely to exceed the vibrational estimate of twice the  $B(E2; 2_1^+ \rightarrow 0_1^+)$  implies that the 691-keV transition is predominantly a  $M1$  transition. Variation of the unknown  $E2$  strength between 0 and 20 W.u. introduces an uncertainty in the final matrix elements of less than 8%. Unknown quadrupole moments of the  $2_1^+$  and the  $2_2^+$  states were varied between the extreme rotational limits which introduces additional uncertainties for the matrix elements of about 1%. The sizes of the resulting matrix elements are insensitive to the choice of their signs within the statistical uncertainties. The mean values of the final results are derived assuming a pure  $M1$   $2_2^+ \rightarrow 2_1^+$  transition and vanishing quadrupole moments, while the estimated uncertainties account for the variations of these quantities. The final results are

$$\begin{aligned} B(E2; 2_2^+ \rightarrow 0_1^+) &= 0.5(2) \text{ W.u.}, \\ B(M1; 2_2^+ \rightarrow 2_1^+) &= 5.4(3.5) \mu_N^2. \end{aligned}$$

The extremely large  $B(M1)$  value is due mostly to the branching ratio reported in Ref. [26]. The large uncertainty in the  $B(M1)$  value is also dominated by the uncertainty of the branching ratio [26]. However, if the real branching ratio is lower by  $1 \sigma$  with respect to the value reported in Ref. [26], the resulting  $B(M1)$  value will be comparable with the highest  $M1$  strengths observed between one-phonon FS and MSS [14]. In this respect the deduced  $B(M1; 2_2^+ \rightarrow 2_1^+) = 5.4(3.5) \mu_N^2$

value can only serve as an indicator that the  $2_2^+$  state in  $^{132}\text{Te}$  decays with a strong  $M1$  transition to the  $2_1^+$  state which qualifies the  $2_2^+$  state as the one-phonon MSS in  $^{132}\text{Te}$ . On the other hand, due to the use of a low- $Z$  target the excitation processes are predominantly one step. Therefore, the result obtained for the  $B(E2; 2_2^+ \rightarrow 0_1^+)$  value, which is also the primary fitting parameter in the Coulomb excitation code, is more reliable. We have not observed the 1665-keV transition in our data, but from the detection limit (see, e.g., Ref. [29]) at 1665 keV we obtained a lower limit for  $I_\gamma(691 \text{ keV})/I_\gamma(1665 \text{ keV}) > 4.2$ . Replacing the branching ratio of the  $2_2^+$  state from Ref. [26] with the calculated lower estimate we establish the lower limit of  $B(M1; 2_2^+ \rightarrow 2_1^+) > 0.23 \mu_N^2$ . This value was obtained entirely on the basis of the current data. Even this lower limit for the  $B(M1; 2_2^+ \rightarrow 2_1^+)$  value clearly shows that the  $2_2^+$  state of  $^{132}\text{Te}$  at 1665 keV is the one-phonon MSS.

With two proton and two neutron holes away from the double magic nucleus  $^{132}\text{Sn}$ ,  $^{132}\text{Te}$  is a natural candidate to be studied within the realistic shell-model framework, which has proved to be a valuable tool to investigate nuclei in this region (see Ref. [30] and references therein). Calculations have been performed along these lines, focusing on the structure of the  $2^+$  states. We consider  $^{132}\text{Sn}$  as a closed core and let the valence protons and neutron holes occupy the five levels  $0g_{7/2}$ ,  $1d_{5/2}$ ,  $1d_{3/2}$ ,  $2s_{1/2}$ , and  $0h_{11/2}$  of the 50–82 shell. The single-particle and single-hole energies have been taken from the experimental spectra of  $^{133}\text{Sb}$  and  $^{131}\text{Sn}$  [31], respectively. The only exception is the proton  $\epsilon_{s_{1/2}}$  which has been taken from Ref. [32], since the corresponding single-particle level is still missing in the spectrum of  $^{133}\text{Sb}$ . Our adopted values for the proton single-particle energies are (in MeV)  $\epsilon_{g_{7/2}} = 0.0$ ,  $\epsilon_{d_{5/2}} = 0.962$ ,  $\epsilon_{d_{3/2}} = 2.439$ ,  $\epsilon_{h_{11/2}} = 2.793$ , and  $\epsilon_{s_{1/2}} = 2.800$ , and for the neutron single-hole energies  $\epsilon_{d_{5/2}}^{-1} = 0.0$ ,  $\epsilon_{h_{11/2}}^{-1} = 0.065$ ,  $\epsilon_{s_{1/2}}^{-1} = 0.332$ ,  $\epsilon_{d_{3/2}}^{-1} = 1.655$ , and  $\epsilon_{g_{7/2}}^{-1} = 2.434$ . For the  $h_{11/2}$  neutron-hole level we have taken the position suggested in Ref. [33].

The two-body component of the effective Hamiltonian has been derived within the framework of perturbation theory [34] starting from the CD-Bonn  $NN$  potential [35] renormalized by way of the  $V_{\text{low-}k}$  approach [36] with a cutoff momentum of  $\Lambda = 2.2 \text{ fm}^{-1}$ . More precisely, we make use of the  $\hat{Q}$ -box folded-diagram expansion including all diagrams up to second order in the interaction, which is taken as the low-momentum potential, plus the Coulomb force for protons. The diagrams of the  $\hat{Q}$  box are computed within the harmonic-oscillator basis using intermediate states composed of all possible hole states and particle states restricted to the five proton and neutron shells above the Fermi surface. This guarantees stability of the results when increasing the number of intermediate states. The oscillator parameter is  $7.88 \text{ MeV}$  as obtained from the expression  $\hbar\omega = 45A^{-1/3} - 25A^{-2/3}$ . The effective proton-neutron and neutron-neutron interactions are derived directly in the particle-hole and hole-hole representation, respectively, while for the proton-proton interaction we use the particle-particle formalism. The shell-model calculations were performed using the OXBASH computer code [37].

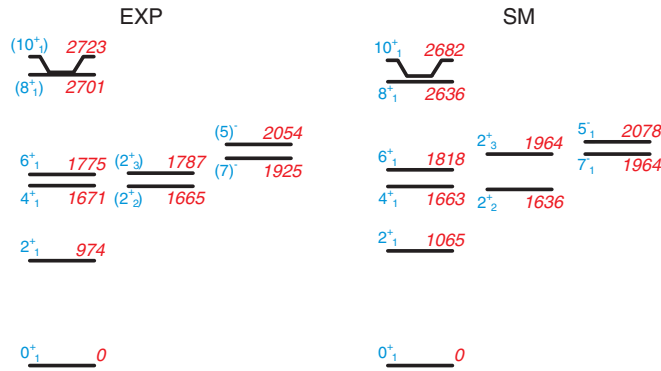


FIG. 2. (Color online) The experimental [26] (EXP) and the calculated (SM) spectra of low-lying states of  $^{132}\text{Te}$ .

Our effective interaction was tested on several nuclei in the mass range of  $^{132}\text{Sn}$ , giving a good description of their spectroscopic properties. However, the agreement between experiment and theory obtained for  $^{130}\text{Sn}$  in the  $N = 82$  neutron shell, with two neutron holes, is not as good as that for  $^{134}\text{Te}$  with two proton particles. The calculated excited states in the former all lie above the experimental ones by about 250–300 keV, while for the latter the discrepancy between calculated and experimental energies is at most 80 keV, except for the second  $2^+$  state, where it reaches 200 keV. Since we are focusing here on FS and MS states of  $^{132}\text{Te}$ , it may be convenient to have the same quality in the description of the proton and neutron systems. To this end, we have reduced the  $J^\pi = 0^+$  neutron-neutron matrix elements by a factor of 0.9 and found that the agreement between theory and experiment in  $^{130}\text{Sn}$  improves substantially. The discrepancy in the energies becomes at most 100 keV.

The calculated energy spectrum of low-lying states of  $^{132}\text{Te}$  is compared with experimental data in Fig. 2. The shell-model calculations reproduce the ordering and the excitation energies of the states. The largest deviations between the calculated energies and the experimental data are 91 keV for the  $2_1^+$  state and 177 keV for the  $2_3^+$  state while for the other states the deviations are less than 50 keV. The calculated and the experimental electromagnetic properties of  $2_1^+$  and  $2_2^+$  states are summarized in Table I. The  $E2$  transition rates have been calculated using effective proton and neutron charges of  $1.7e$  and  $0.7e$ , respectively, which lead to  $B(E2)$  values for  $^{134}\text{Te}$  and  $^{130}\text{Sn}$  quite close to experiment. As regards the magnetic properties, we have used free orbital neutron and proton  $g_l$  factors, while the free  $g_s$  factors are both multiplied by 0.7. With this choice, which corresponds to the most commonly adopted one, we can also reproduce the magnetic moments of the yrast  $6^+$  states of  $^{134}\text{Te}$  and  $^{132}\text{Te}$  [38].

All the experimental values in Table I are well reproduced except the  $B(M1; 2_2^+ \rightarrow 2_1^+)$  strength for which the calculations reproduce only the lower limit. We have verified that this is also the case when using matrix elements of the effective  $M1$  operator, which, consistently with the two-body interaction, are derived at second order in perturbation theory. By adjusting the effective gyromagnetic factors, the calculated  $B(M1; 2_2^+ \rightarrow 2_1^+)$  can be raised up to  $0.35\text{--}0.50 \mu_N^2$  under the condition that the experimental  $\mu(2_1^+)$  is also reproduced

TABLE I. Comparison of the available experimental data on the electromagnetic properties of the  $2_1^+$  and the  $2_2^+$  states in  $^{132}\text{Te}$  with results of the shell-model calculations.

Observable	Unit	Experiment	Shell Model
$B(E2; 2_1^+ \rightarrow 0_1^+)$	W.u.	$10(1)^a$	7.8
$\mu(2_1^+)$	$\mu_N$	$+0.92(10)^b$	0.68
$B(E2; 2_2^+ \rightarrow 0_1^+)$	W.u.	$0.5(1)^c$	0.21
$B(E2; 2_2^+ \rightarrow 2_1^+)$	W.u.	$0\text{--}20^c$	0.24
$B(M1; 2_2^+ \rightarrow 2_1^+)$	$\mu_N^2$	$5.4(3.5)^c (>0.23^d)$	0.20
$\mu(2_2^+)$			0.69

<sup>a</sup>From Ref. [1] and the present work.

<sup>b</sup>From Refs. [8,9] and the present work.

<sup>c</sup>From the Coulomb excitation analysis in this work and the branching ratio of the decay of  $2_2^+$  from Ref. [26].

<sup>d</sup>From the Coulomb excitation analysis and the detectability limit for 1665-keV transition in this work.

(Table I). We present here the shell-model results obtained with the commonly used gyromagnetic factors. Even with these gyromagnetic factors (see Table I) the calculated  $B(M1; 2_2^+ \rightarrow 2_1^+)$  value is large enough to firmly conclude that the  $2_2^+$  state of  $^{132}\text{Te}$  is the one-phonon MSS.

The MS character of the calculated  $2_2^+$  state of  $^{132}\text{Te}$  is evident from the structure of its wave function too. In terms of the basic  $2^+$  proton and neutron excitations the shell-model wave functions of the ground and the two lowest lying  $2^+$  states can be presented as follows:

$$|0_1^+\rangle = 0.94|0_1^+\rangle_\nu|0_1^+\rangle_\pi + \dots, \quad (1)$$

$$|2_1^+\rangle = 0.66|0_1^+\rangle_\nu|2_1^+\rangle_\pi + 0.62|2_1^+\rangle_\nu|0_1^+\rangle_\pi + \dots, \quad (2)$$

$$|2_2^+\rangle = 0.58|0_1^+\rangle_\nu|2_1^+\rangle_\pi - 0.63|2_1^+\rangle_\nu|0_1^+\rangle_\pi + \dots, \quad (3)$$

where  $\pi(\nu)$  denote the respective excitations in  $^{134}\text{Te}$  ( $^{130}\text{Sn}$ ) and “ $\dots$ ” means minor components. Equations (2) and (3) indicate almost equal proton and neutron contributions to the  $2_1^+$  and the  $2_2^+$  states of  $^{132}\text{Te}$ ; i.e., no CIP is present. This is due to almost equal energies of the basic  $2^+$  proton [ $E_x(2_1^+; ^{134}\text{Te}) = 1279$  keV] and neutron [ $E_x(2_1^+; ^{130}\text{Sn}) = 1221$  keV] configurations which even in the case of very weak proton-neutron interaction leads to one-phonon  $2^+$  states with a balanced proton-neutron character. The main difference between Eqs. (2) and (3) is the opposite sign of the neutron and proton components of the wave function of the  $2_2^+$  state [see Eq. (3)] which makes it antisymmetric with respect to interchanges of proton and neutron components in the wave function. Equation (3) represents a shell-model wave function which describes a MSS. The isovector character of this wave function leads to the relatively large  $B(M1; 2_2^+ \rightarrow 2_1^+)$  value. The shell-model calculations confirm the nature of the two lowest lying  $2^+$  states of  $^{132}\text{Te}$  as FS and MS states, respectively, with balanced neutron and proton components. This provides confidence in the reliability of the model when applied to the more exotic nucleus  $^{136}\text{Te}$ . It is of great interest to study the proton-neutron balance in the wave functions of the one-phonon states of  $^{136}\text{Te}$  where the effect of CIP is expected to be more pronounced than in the case of  $^{132}\text{Te}$ .

In summary, by using the data from a projectile Coulomb excitation experiment we have identified the  $2_2^+$  state of  $^{132}\text{Te}$  as the one-phonon MSS. This is the first case of a MSS of an unstable, neutron-rich nucleus identified on the basis of a large absolute  $M1$  transition strength. The experimental results prove that projectile Coulomb excitation experiments on light targets are an appropriate technique to study MSSs of exotic nuclei. The performed shell-model calculations based on the  $V_{\text{low-}k}$  interaction successfully reproduce the experimental data and the isovector character of the  $2_2^+$  state of  $^{132}\text{Te}$ . The shell-model wave functions of the one-phonon states have a balanced proton-neutron character as expected from the evolution of collectivity in

the neutron-rich tellurium isotopes around the  $N = 82$  shell closure.

G.R. is supported by the Alexander von Humboldt Foundation. This manuscript has been authored by UT-Battelle, LLC, under Contract No. DE-AC05-00OR22725 with the US Department of Energy. This work was supported by the DFG (Grants No. Pi 393/2-2 and No. SFB 634), by the German-Bulgarian exchange program (Grant No. PPP 50751591), by the BgNSF (Grant No. DO 02-219), by the HIC for FAIR, by the Office of Nuclear Physics, US Department of Energy, Grant No. DE-FG02-96ER40983, and by the ARC, Grant No. DP0773273.

- 
- [1] D. C. Radford *et al.*, *Phys. Rev. Lett.* **88**, 222501 (2002).  
 [2] L. Grodzins, *Phys. Lett.* **2**, 88 (1962).  
 [3] R. F. Casten, *Nucl. Phys. A* **443**, 1 (1985).  
 [4] J. Terasaki, J. Engel, W. Nazarewicz, and M. Stoitsov, *Phys. Rev. C* **66**, 054313 (2002).  
 [5] N. Shimizu, T. Otsuka, T. Mizusaki, and M. Honma, *Phys. Rev. C* **70**, 054313 (2004).  
 [6] A. Covello, L. Coraggio, A. Gargano and N. Itaco, *Prog. Part. Nucl. Phys.* **59**, 401 (2007).  
 [7] N. J. Stone *et al.*, *Phys. Rev. Lett.* **94**, 192501 (2005).  
 [8] A. E. Stuchbery and N. J. Stone, *Phys. Rev. C* **76**, 034307 (2007).  
 [9] N. Benczer-Koller *et al.*, *Phys. Lett. B* **664**, 241 (2008).  
 [10] N. Lo Iudice and F. Palumbo, *Phys. Rev. Lett.* **41**, 1532 (1978).  
 [11] F. Iachello, *Phys. Rev. Lett.* **53**, 1427 (1984).  
 [12] J. D. Holt, N. Pietralla, J. W. Holt, T. T. S. Kuo, and G. Rainovski, *Phys. Rev. C* **76**, 034325 (2007).  
 [13] V. Werner *et al.*, *Phys. Rev. C* **78**, 031301(R) (2008).  
 [14] N. Pietralla, P. von Brentano, and A. F. Lisetskiy, *Prog. Part. Nucl. Phys.* **60**, 225 (2008), and references therein.  
 [15] B. Fazekas *et al.*, *Nucl. Phys. A* **548**, 249 (1992).  
 [16] I. Wiedenhöver *et al.*, *Phys. Rev. C* **56**, R2354 (1997).  
 [17] N. Pietralla *et al.*, *Phys. Rev. C* **58**, 796 (1998).  
 [18] T. Ahn *et al.*, *Phys. Lett. B* **679**, 19 (2009).  
 [19] G. Rainovski *et al.*, *Phys. Rev. Lett.* **96**, 122501 (2006).  
 [20] T. Ahn *et al.* (unpublished).  
 [21] L. Coquard *et al.*, *Phys. Rev. C* **82**, 024317 (2010).  
 [22] J. Iwanicki *et al.*, ISOLDE experiment IS423, completed 2008, unpublished.  
 [23] G. Rainovski *et al.*, GSI experiment U242, completed 2010, unpublished.  
 [24] J. Sau and K. Heyde, *Phys. Rev. C* **23**, 2315 (1981).  
 [25] K. Sieja, G. Martinez-Pinedo, L. Coquard, and N. Pietralla, *Phys. Rev. C* **80**, 054311 (2009).  
 [26] R. O. Hughes *et al.*, *Phys. Rev. C* **71**, 044311 (2005).  
 [27] C. J. Gross *et al.*, *Nucl. Instrum. Methods Phys. Res. A* **450**, 12 (2000).  
 [28] K. Alder and A. Winther, *Coulomb Excitation* (Academic Press, New York, 1966).  
 [29] G. F. Knoll, *Radiation Detection and Measurement*, 3rd ed. (John Wiley & Sons Inc., New York, 2000).  
 [30] A. Covello, L. Coraggio, A. Gargano, and N. Itaco, *J. Phys. Conf. Ser.* **267**, 012019 (2011).  
 [31] Data extracted using the NNDC Online Data Service from the ENSDF database, file revised as of May 23, 2011.  
 [32] F. Andreozzi, L. Coraggio, A. Covello, A. Gargano, T. T. S. Kuo, and A. Porrino, *Phys. Rev. C* **56**, R16 (1997).  
 [33] B. Fogelberg *et al.*, *Phys. Rev. C* **70**, 034312 (2004).  
 [34] L. Coraggio, A. Covello, A. Gargano, N. Itaco, and T. T. S. Kuo, *Prog. Part. Nucl. Phys.* **62**, 135 (2009), and references therein.  
 [35] R. Machleidt, *Phys. Rev. C* **63**, 024001 (2001).  
 [36] S. Bogner, T. T. S. Kuo, L. Coraggio, A. Covello, and N. Itaco, *Phys. Rev. C* **65**, 051301 (2002).  
 [37] B. A. Brown, A. Etchegoyen, and W. D. M. Rae, computer code OXBASH, MSU-NSCL, Report No. 534.  
 [38] N. J. Stone, *At. Data Nucl. Data Tables* **90**, 75 (2005).